POLE PLACEMENT CONTROLLER BASED ON ROBUST INTERNAL-LOOP COMPENSATOR FOR HIGH-ACCURACY LINEAR MOTION SYSTEM

Seong-Hyun Jeong, Jung-Il Park and Suk-Gyu Lee

School of Electrical Engineering and Computer Science,
Yeungnam University, Gyongbuk, Korea

Abstract: In this paper, the pole placement controller based on the Robust Internal-loop Compensator(RIC) structure, which has inherent structural equivalence to disturbance observer, is proposed to control a linear positioning system. This controller has the advantage to easily select controller gains by using pole placement without loss of that of original RIC structure. The principal is to construct the pole placement controller for a nominal internal model instead of unknown real plant. The effectiveness of the proposed controller is shown by linear motion experiments.

Keywords: Robust Internal-loop Compensator, Pole Placement Controller, Disturbance Observer, Linear Motor, High Accuracy Motion Control.

1. INTRODUCTION

In order to convert the rotating motion to the translational motion, there are two ways using the ball screw structure(Ohmae *et al*., 1987; Lee, and Tomizuka, 1996) or getting linear motion directly with linear motor(Gerco, *et al*., 1997; Kwon, and Park, 2000; Kim, and Chung, 2001; Xu, and Yao 2001) without ball screw structure. In the ball screw positioning system, there are difficulties obtaining high accuracy because of nonlinearity such as backlash due to gears. The linear motion system using linear motor makes it also difficult to obtain high accuracy because of applying external disturbance directly due to the direct drive structure. In order to enhance the accuracy of the positioning system, the ways by using the disturbance observer technique(Ohmae *et al*., 1987; Lee, and Tomizuka, 1996) and the using neural networks(Gerco, *et al*., 1997; Kwon, and Park, 2000) have been utilized.

Recently, the linear motion system adopting linear motor is increasing in industrial field. The learning feedforward controller using neural network was announced to obtain high accuracy of the position system adopting linear synchronous motor(Gerco, *et al*., 1997) and the same structure was also applied into the linear motion system with linear pulse motor(Kwon, and Park, 2000). The studies to design the robust controller for disturbances and uncertainty were announced(Kim, and Chung, 2001, 2002, 2003; Xu, and Yao, 2002). The fact that the conventional disturbance observer structure is equivalent to the robust Internal-loop compensator(RIC) was known (Kim, and Chung, 2001). The RIC structure proposed by Kim and Chung (2002) is also similar to the internal model control(IMC) (Zhu, *et al*., 1995) structure from point of view that it is designed for a nominal internal reference model instead of unknown real plant.

The scheme proposed in this paper is the combined structure, the pole placement controller as an outer-loop controller and RIC as an internal-loop controller. The controller proposed by Kim and Chung (2002) has the 1st order closed loop characteristic, this gives slow response for step input. To overcome this, the method to enhance the transient response by using pole placement controller is proposed. Using a linear motion experiment showed the effectiveness of the

proposed controller.

2. POLE PLACEMENT CONTROLLER USING RIC STRUCTURE

2.1 RIC Structure

The structure of an original robust internal-loop compensator is shown in Fig. 1. $P(s)$ is the transfer function of plant, y is the output signal of plant, u_r is the reference control input, $P_m(s)$ is the reference plant model, and y_r is the reference output signal, respectively. d_{ex} is the external disturbance, the measurement noise ξ is added in the output signal. From Fig.1, the control input is calculated as follows:

$$u = u_r + K(s)e_r \tag{1}$$

where $K(s)$ is the feedback compensator in internal-loop.

The equivalent RIC structure of Fig.1 can be changed as shown in Fig. 2(Kim, and Chung, 2001, 2002). Comparing Fig. 1 with Fig. 2, $Q(s)$ is obtained in the following equation

$$Q(s) = \frac{P_m(s)K(s)}{1 + P_m(s)K(s)} \tag{2}$$

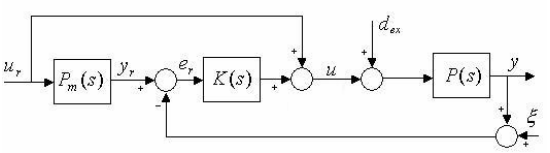

Fig. 1. Robust internal-loop compensator

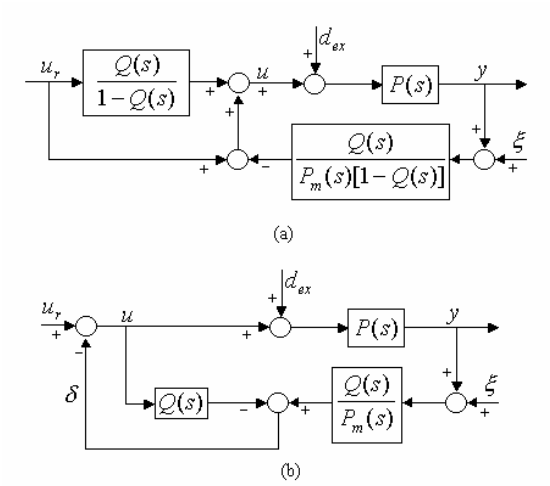

Fig. 2. Equivalent structure of RIC (a) RIC structure using Q function (b) DOB with reference model $P_m(s)$

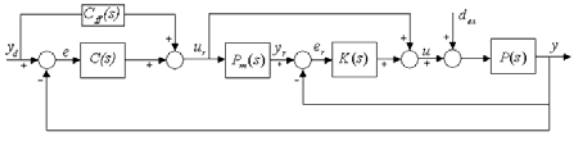

Fig. 3. Overall control system and RIC

The structure of Fig. 2 (a) is the same as RIC structure of Fig. 1, the structure of Fig. 2 (b) is a typical DOB(Disturbance observer), hence the RIC structure is equivalent to the DOB. Many studies to design Q filter of DOB structure have been researched(Lee, and Tomizuka, 1996; Kim, and Chung, 2001, 2002) . In the RIC structure, how to design K(s) becomes a key point. The details for this and robust stability were described by Kim and Chung, (2001, 2002). The external controller was designed as an internal-loop controller by using the dual RIC structure. The final structure is shown in Fig. 3. $C_{ff}(s)$ is the feedforward controller, and $C(s)$ is the feedback controller.

2.2 Design of computed torque-like controller

In general, the internal-loop compensator, DOB, is designed to eliminate the uncertain disturbance. The outer-loop feedback controller is designed after the internal-loop controller is designed in advance.

$P_m(s)$ in Fig. 3 and $K(s)$ of the equation (1) are selected as

$$P_m(s) = \frac{1}{J_m s^2 + B_m s},\ K(s) = \left[\frac{1}{P_m(s)}\right]\frac{\Lambda(s)}{s} \tag{3}$$

where, J_m and B_m are the mass of internal model and the friction coefficient, respectively. If $D(s)$ is constant, $K(s)$ becomes the PD controller. Q(s) of this controller from equation (2) is given by

$$Q(s) = \frac{D(s)}{s + D(s)} \tag{4}$$

Now let's design the outer-loop controller $C(s)$. If $C(s)$ is chosen as same type as $K(s)$, the reference control input is obtained as

$$\begin{aligned} u_r &= C_{ff}(s)y_d + C(s)e \\ &= \frac{1}{P_m(s)}\left[y_d + \frac{\Lambda(s)}{s}e\right] \end{aligned} \tag{5}$$

where, $C_{ff}(s) = J_m s^2 + B_m s$,

$$C(s) = \left[\frac{1}{P_m(s)}\right]\frac{\Lambda(s)}{s} = (J_m s + B_m)\Lambda(s) \tag{6}$$

Then the final robust control input is given by Kim, and Chung(2001, 2002).

$$u = J_m[s^2 y_d + \Lambda(s)se] + B_m[sy_d + \Lambda(s)e] + K(s)e_r \tag{7}$$

$$\text{where, } e_r = \left[1 + \frac{\Lambda(s)}{s}\right]e \tag{8}$$

2.3 PD controller design based on pole placement

As discussed earlier, when the control input is calculated, how to choose $\Lambda(s)$ is key point. That is

done by the Q filter design method of conventional DOB structure from equation (5). In the work by Kim and Chung(2001, 2002), $\Lambda(s)$ was selected as constant to make the PD controller. If K(s) in the internal-loop is very big and works well, the transfer function of RIC in the internal-loop becomes $P_m(s)$. Then the poles of total closed loop characteristic equation is given by

$$1 + C(s)P_m(s) = 1 + \frac{\Lambda(s)}{s} = 0 \tag{9}$$

From equation (9), if $\Lambda(s)$ is chosen as constant, the characteristic equation becomes 1st order system. The constant $\Lambda(s)$ makes it easy to choose the gains to calculate the control input. In the work by Kim and Chung(2001), as both the internal-loop and the outer-loop controller $\Lambda(s)$ were selected as constant, hence the controllers become PD controller. In this case, the closed-loop characteristic becomes 1st order system. This makes it difficult to obtain a fast response for step input which has high frequencies and good transient response. To overcome this, in this paper, the internal-loop controller K(s) is designed in the same manner as the original method, whereas the outer-loop controller C(s) is designed using the pole placement.

The proposed control input is expressed as follows:

$$\begin{aligned} u &= C_{ff}(s)y_d + C(s)e + Ke_r \\ &= J_m s^2 y_d + B_m s y_d + C_1 s\Lambda e + C_2 \Lambda e + K(s)e_r \end{aligned} \tag{10}$$

where,

$$C_{ff}(s) = J_m s^2 + B_m s \ , \ C(s) = (C_1 s + C_2)\Lambda$$

$$e_r = \left[1 + \frac{\Lambda(s)}{s}\right] e$$

$$K(s) = \left[\frac{1}{P_m(s)}\right]\frac{D}{s} = (J_m s + B_m)D$$

here, Λ, D, C_1, C_2 are constant.

If the internal-loop works as reference plant model, the characteristic equation of the closed-loop becomes 2nd order system as

$$s^2 + 2\varsigma\omega_n s + {\omega_n}^2 = 0 \tag{11}$$

where, ς is the damping ratio, and ω_n is the natural frequency. After choosing both ς and ω_n which has the desired transient response, the outer-loop controller's gain, C_1 and C_2 , are calculated by using the pole placement technique.

The characteristic equation of closed loop using same method similar to equation (9) is given by

$$1 + C(s)P_m(s) = 1 + (K_1 s + K_2)\Lambda\left(\frac{K_t}{J_m s^2 + B_m s}\right) = 0 \tag{12}$$

Equation (12) can be rearranged as follows

$$s^2 + \frac{B_m + \Lambda K_t C_1}{J_m} s + \frac{\Lambda K_t C_2}{J_m} = 0 \tag{13}$$

Comparing (11) with (13), the gain C_1 and C_2 such that the closed-loop poles are placed on desired points are obtained in the following equation

$$C_1 = \frac{2\varsigma\omega_n J_m - B_m}{\Lambda K_t}, \ C_2 = \frac{J_m {\omega_n}^2}{\Lambda K_t} \tag{14}$$

2.4 Robust stability condition based on RIC

The work by Kim and Chung(2001, 2002) showed that if the model $P_m(s)$ is stable and linear controllers, K and C in the structure of Fig. 3, can stabilize $P_m(s)$ for the uncertainty ΔP expressed as $P = P_m(1 + \Delta P)$.

3. EXPERIMENTAL RESULTS

3.1 Measurement of basic characteristics for motion control

The linear motion system used in motion control is the 「LW7-20」 stage(Anorad Corp.) This consists of a linear synchronous motor which has 340 [N]peak force and a linear encoder of 0.5[um] resolution to measure position. The stroke is 508 [mm]. The servo driver is 「SMA8415-1A-1」 (GLENTEK Corp.) which has 25 [A] peak current. The DSP board embedded TMSC320C31 is used as a controller. Figure 4 shows the overall block diagram of experimental system.

Before performing motion controls, the basic dynamics(motor torque constant, viscous friction) of the linear motor system is measured in advance. Without feedback, the step input is applied into the system shown in equation (15), and then the velocity of the system is expressed as equation (16).

$$P_\omega(s) = \frac{K_t}{Js + B} \tag{15}$$

$$\omega(t) = \frac{K_t}{B}\left(1 - e^{-t/\tau}\right) \tag{16}$$

where, time constant $\tau = J/B$ (17)

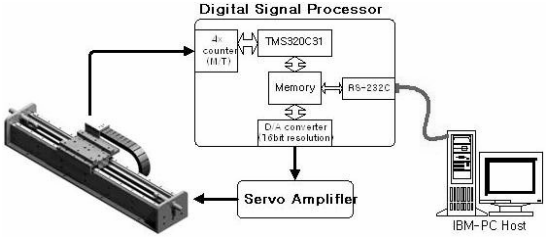

Fig. 4. Overall block diagram of experimental system.

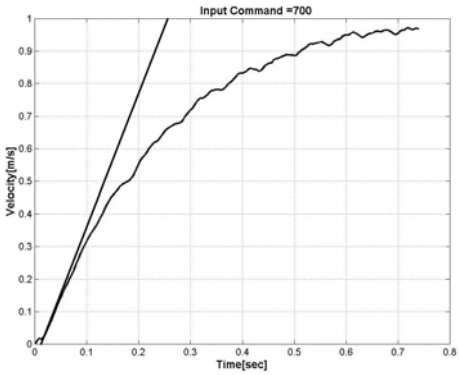

Fig. 5. Output characteristic for step input 700(= 1.7[V]).

When the step input 1.7 V is applied into real linear motor system through D/A converter, the step response is measured as shown in Fig. 5. Since the steady state final value is about 1 [m/sec], the time constant is about 0.25[sec], the equations (16), (17) are given by

$$\omega(t) = \frac{r \cdot K_t}{B} = 1 \tag{18}$$

here r is the magnitude of step input.

$$\tau = J/B = 0.25 \tag{19}$$

The mass of the moving part is measured as 2.5[Kg]. From all these, the following characteristic values are obtained as

$$J = 2.5[Kg],\ B = 10[Kg/\sec],\ K_t = 5.8514[N/V] \tag{20}$$

3.2 Motion control and results

In the experiment, the step input and motion input according to profile are used, respectively. The additional experiments were performed to show the robustness of the proposed controller.

Experiment for step input

The conditions used in the step input experiment are chosen as equation (20). Λ is 5 and D is 10,000. In the original method, $K(s)$ and $C(s)$ becomes 2.5s+10(= $J_m s + B_m$). In the case of the proposed pole placement controller, the gains are chosen by using equations (14) and (20) with the natural frequency(ω_n) is 60 [rad/sec], damping ratio(ς) is 0.9.

The result of the step input is shown in Fig. 6. In the case of the original controller, the response is shown as 1st order response. Since Λ is 5, the time constant of closed loop system is about 0.2 second. In the case of the proposed controller, the closed-loop system responds as 2nd order system. The output response shape in the case of damping ratio ς is 0.9, there is some overshoot, about 30% overshoot occurred. This might be a result of the internal-loop not being exactly equal to $P_m(s)$. In the case of the proposed controller, if the natural frequency and the damping ratio were chosen properly, then the better transient response can be obtained.

Experiment for profile input

Now the responses are measured for the motion profile which is shown in Fig. 7. The results are compared for both methods. Figure 7 shows the shapes of profile for position, velocity and acceleration. The motion is round movement between 5[cm] range. The maximum acceleration is $2.5m/\sec^2$. The experimental conditions are the same as the above experiment except that Λ is 5, D is 20,000, natural frequency is 140 [rad/sec], and the damping ratio is 0.9. The results of this case are shown in Fig. 8. Figure 8 depicts that the RIC structure using the proposed pole placement technique shows the better performance than the original RIC under the same conditions. The position errors are within ±40 [um]. So, the other motion control experiments were performed by using the pole placement controller according to various natural frequencies and damping ratios. Figure 9 shows the results according to natural frequency 60, 140 [rad/s] respectively. Figure 10 shows the results according to damping ratio 0.5, 3, respectively.

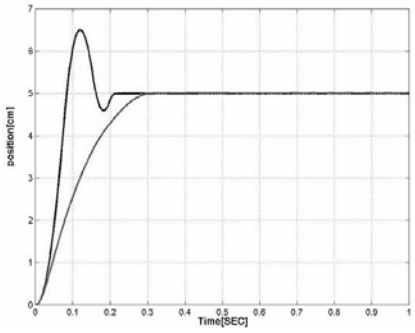

Fig. 6. Comparison output responses using original RIC and pole placement based on RIC for step reference input ($\Lambda = 5.0, \omega_n = 60, \ \varsigma = 0.9$, $D = 10{,}000$).

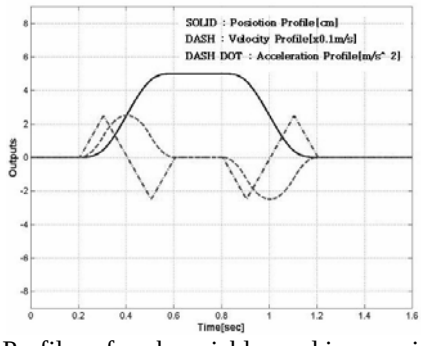

Fig. 7. Profiles of each variable used in experiment.

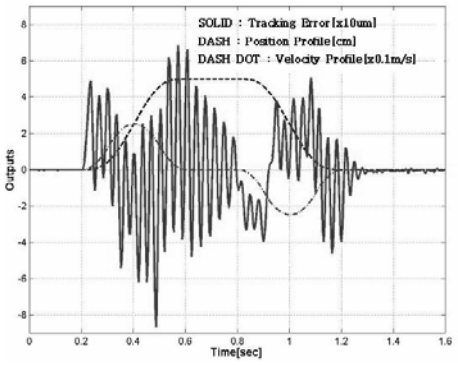

(a) Original RIC

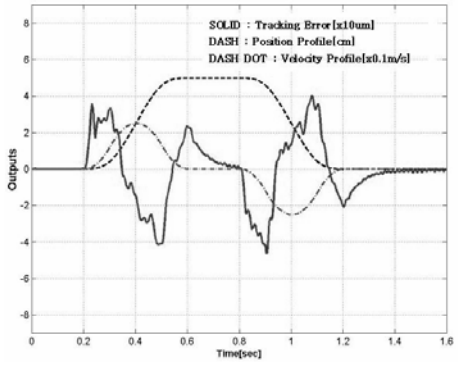

(b) Pole placement based on RIC

Fig. 8. Comparison of position errors for each controller.

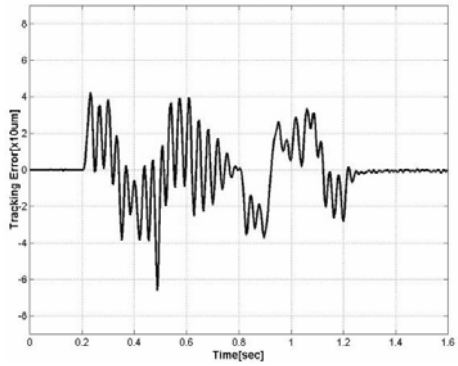

(a) $\omega_n = 60,\ \varsigma = 0.9,\ D = 12{,}000$

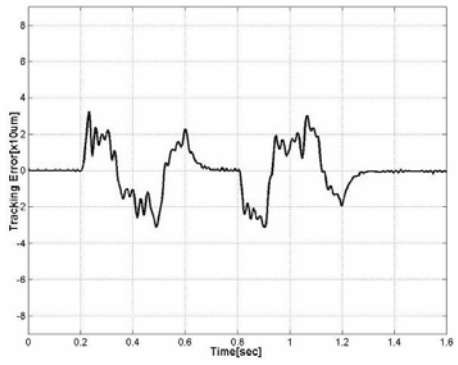

(b) $\omega_n = 140,\ \varsigma = 0.9,\ D = 12{,}000$

Fig. 9. Comparison of position errors according to various natural frequency for pole placement based RIC on controller.

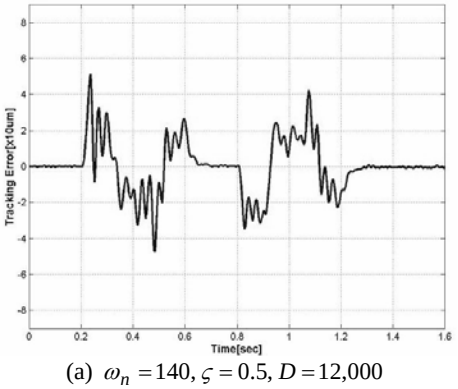

(a) $\omega_n = 140,\ \varsigma = 0.5,\ D = 12{,}000$

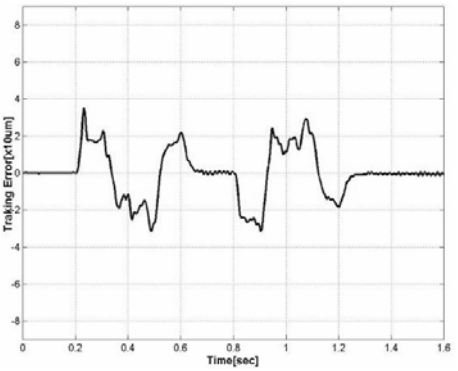

(b) $\omega_n = 140,\ \varsigma = 3.0,\ D = 12{,}000$

Fig. 10. Comparison of position errors according to various damping ratio for pole placement based RIC on controller.

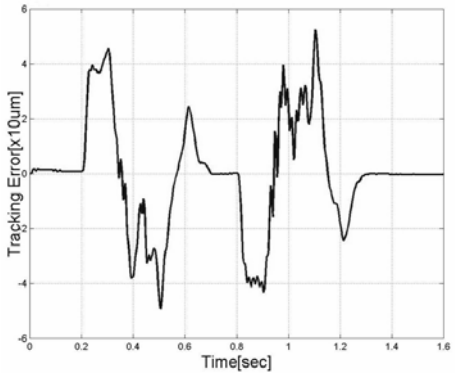

(a) $J_m = 2.5,\ B_m = 5$

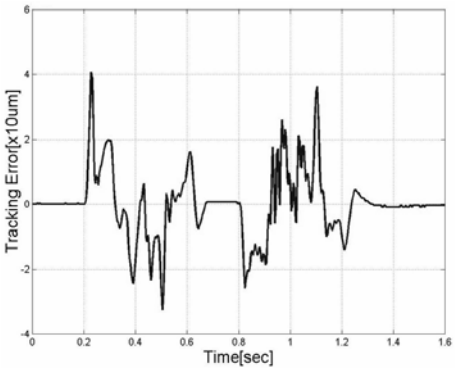

(b) $J_m = 2.5,\ B_m = 15$

Fig. 11. Comparison of position errors according to parameters variations of internal model for pole placement based RIC on controller.(Cont.)

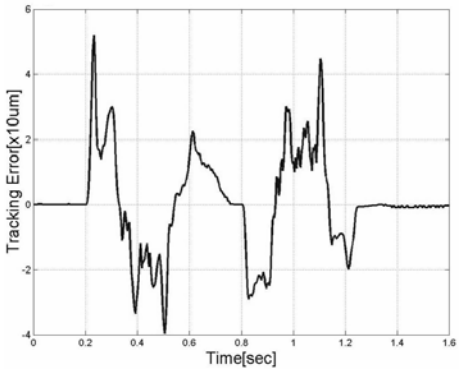

(c) $J_m = 1.0,\ B_m = 10$

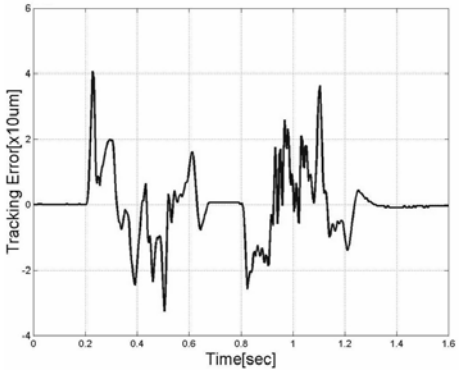

(d) $J_m = 3.0,\ B_m = 10$

Fig. 11. Comparison of position errors according to parameters variations of internal model for pole placement based RIC on controller.

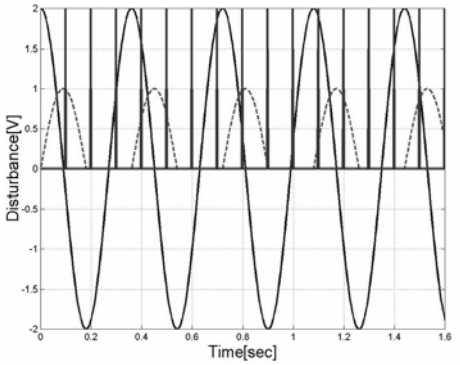

(a) Disturbances

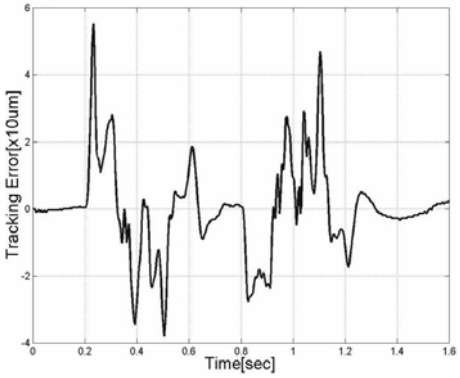

(b) Position tracking error

Fig. 12. Position error in the presence of the external disturbances.

Additional Experiment to show robustness

Figure 11 shows the position error according to parameters variations of internal model. The robustness property of the proposed controller under the parameter variations of internal model was verified. The experimental conditions are as follows: Λ is 5, D is 20,000, natural frequency is 140 [rad/sec], and the damping ratio is 0.9.

Figure 12 shows the tracking result in the presence of disturbances. The external disturbances used in the experiment consist of a sinusoid, a half sinusoid, and a series of impulse as shown in Fig. 12(a).

4. CONCLUSIONS

In this paper, the pole placement controller based on the Robust Internal-loop Compensator(RIC) structure, which has inherent structural equivalence to disturbance observer, is proposed to control a linear positioning system. The proposed controller has the advantage to easily select controller gains by using pole placement without loss of that of original RIC structure as choosing the natural frequency and damping ratio for a nominal internal model instead of unknown real plant. The proposed pole placement controller have the better performance than the original RIC through linear motion experiment adopting linear motor. The effectiveness of the proposed controller was shown through the motion experiments for various natural frequencies and damping ratios.

REFERENCES

Gerco Otten, Theo J. A. de Vries, Adrian M. Rankers, and Erik W. Gaal. (1997). *IEEE ASME Trans. on Mechatronics*, Vol.2, No.3, pp. 179-181.

Kim, B. K. and Chung W. K. (2001). *Proc. American Control Conf.*, pp. 4046-4051.

Kim, B. K. and Chung W. K., (2002). *IEEE/ASME Trans. on Mechatronics*, Vol. 7, No.4, pp. 500-514.

Kim, B. K. and Chung W. K. (2003). *IEEE Trans. on Industrial Electronics*, Vol. 50, No.6, pp. 1207-1216, 2003

Kwon. Y .K. and Park J. I. (2000). *Proceedings of the IASTED International Conference on MIC*, pp.49-53.

Lee, H. S. and Tomizuka, M. (1996). *IEEE Trans on. Ind. Electron*., Vol. 43, pp. 48-55.

Ohmae, Matsuda T., Kanno M. and Saito K. (1987). *IEEE Trans.on Ind. Applicat*., Vol. 1A-23, No. 5.

Xu Li and Yao Bin (2001*). IEEE/ASME Trans. on Mechatronics*, Vol. 6, No.4, pp. 444-452.

Zhu H. A., Hong G. S., Teo C. L., and Poo A. N (1995). *Int. J. Syst. Sci*., Vol. 26, No. 2, pp. 277-293.